Microchannel Heat Exchangers Based on Alloy 230 – Exposure Characteristics and Mechanical Behavior

FWP 1022406 –Advanced Alloy Development
Period of performance: 10/1/2016 – 9/30/2017

Ömer N. Doğan
Research & Innovation Center
National Energy Technology Laboratory
1450 Queen Avenue, S.W., Albany, Oregon 97321
omer.dogan@netl.doe.gov

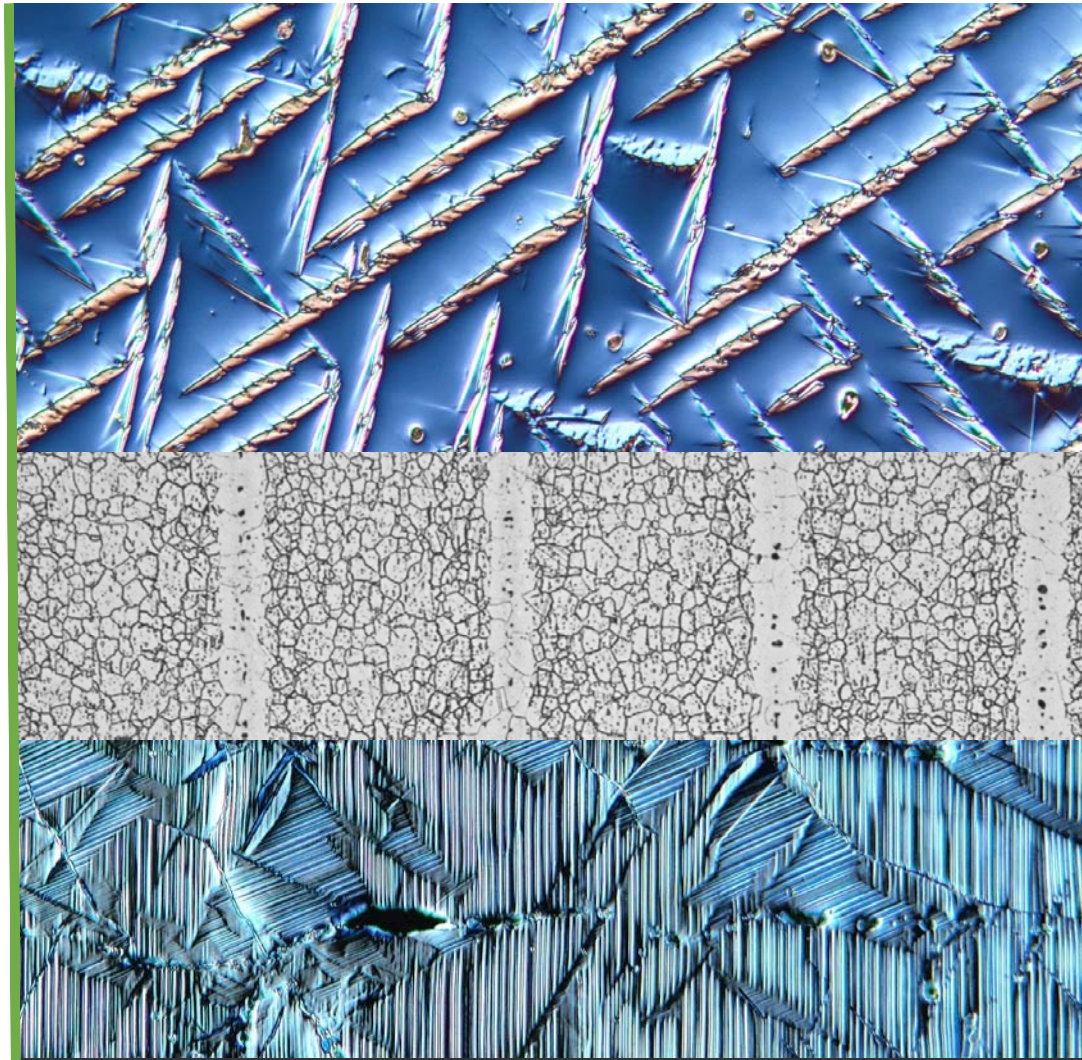

Crosscutting Technology Research Project Review
March 22, 2017 – Pittsburgh, PA

Acknowledgements

Monica Kapoor
Kyle Rozman
Richard Oleksak
Sajedur Akanda

Casey Carney
Jeffrey Hawk
Gordon Holcomb

Rajesh Saranam
Patrick McNeff
Brian Paul

This work was performed in support of the U.S. Department of Energy's Fossil Energy (FE) Crosscutting Technology Research and Advanced Turbines Programs. The research was executed through NETL's Research and Innovation Center's Advanced Alloy Development Field Work Proposal.

Project Goals and Objectives

- **Accelerating commercialization of supercritical carbon dioxide power cycle technology by addressing materials and manufacturing challenges for components of sCO_2 power systems.**
  - Joining of similar and dissimilar power plant alloys
  - Performance of joints in sCO_2 power cycle environments
- **Milestones**
  - Demonstrate mechanical and environmental performance of joints in supercritical CO_2 - 09/30/2017
- **Deliverables**
  - Technical report (either presentation or publication) on the high temperature corrosion of the joined power plant materials. - 09/30/2017
  - Technical report (either presentation or publication) on the cross-joint strength of typical power plant materials. - 09/30/2017

Outline

- **Supercritical CO_2 power cycles and compact heat exchangers**
- **Materials issues in manufacturing compact heat exchangers**
  - Diffusion bonding (DB)
  - Transient liquid phase bonding (TLPB)
- **Mechanical strength of bonded structures**
- **High-temperature corrosion of bonds in sCO_2**

Supercritical CO_2 Power Cycles

NATIONAL ENERGY TECHNOLOGY LABORATORY

Indirect sCO_2 Cycle

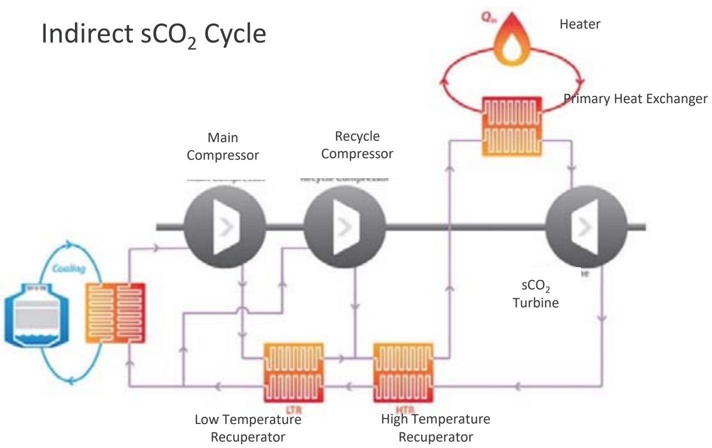

Direct sCO_2 Cycle

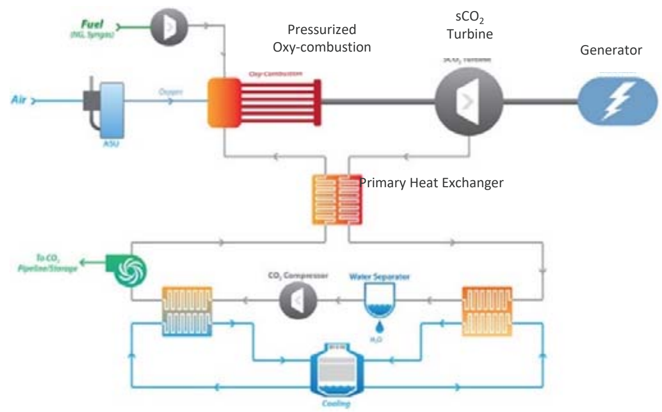

Cycle/Component		Inlet T (C)	Inlet P (MPa)	Outlet T (C)	Outlet P (MPa)
Indirect	Heater	450-535	1-10	650-750	1-10
	Turbine	650-750	20-30	550-650	8-10
	HX	550-650	8-10	100-200	8-10
Direct	Combustor	750	20-30	1150	20-30
	Turbine	1150	20-30	800	3-8
	HX	800	3-8	100	3-8

Essentially pure CO_2

CO_2 with combustion products including O_2, H_2O and SO_2

U.S. DEPARTMENT OF ENERGY

Compact Heat Exchangers for sCO_2 Cycles

NATIONAL ENERGY TECHNOLOGY LABORATORY

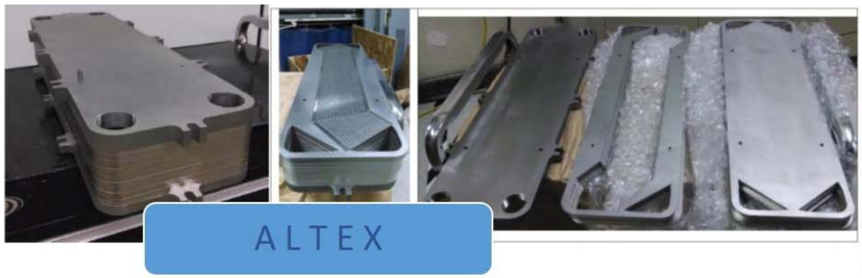

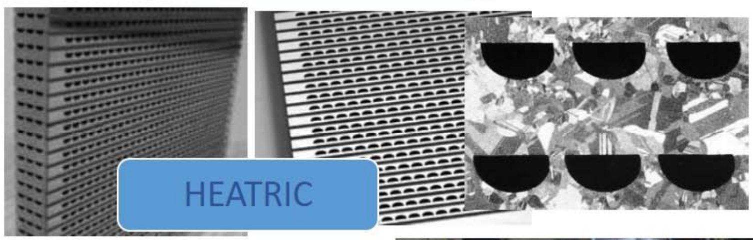

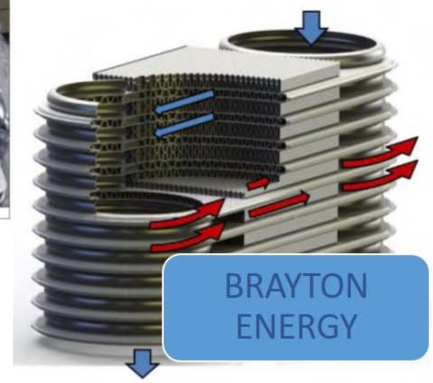

- Higher efficiency
  - Due to much shorter heat diffusion lengths in fluid
- Smaller size
  - Use of less materials (expensive superalloys)
  - Takes less space
- Modular design
  - Expandable to large power plants

Heat Exchangers

Micro channel heat exchangers

- Higher heat transfer efficiency due to shorter heat diffusion lengths
- Smaller size
- Modular Design

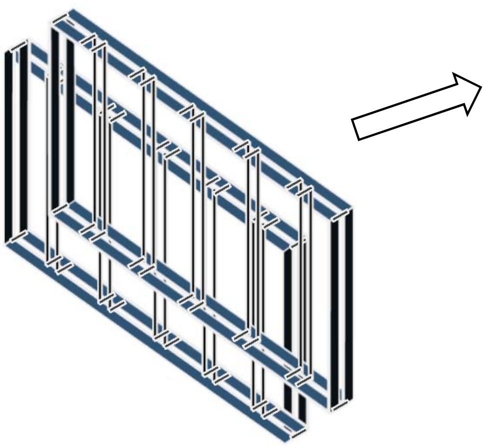

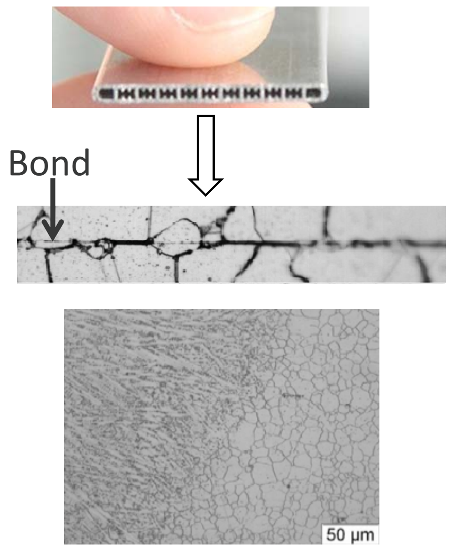

- Dimensional Tolerances
  - Pressure & Temperature Drop
- Uniform microstructure
  - Environmental Resistance

Diffusion bonding, brazing, and transient-liquid-phase (TLP) bonding are the most robust approaches for sCO_2 cycles

- Pattern microscale flow paths
- Join these using laser welding, diffusion bonding or brazing

Microfluidics.com, Basuki et al., MSEA, 538 (2012) 340-348; Zapirain et al. Physics Procedia, 12 (2011) 105-112

Schematic of diffusion bonding process

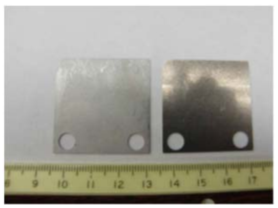

550 µm shims

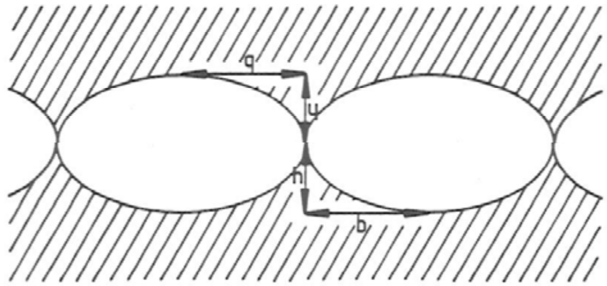

Parallel, elliptical voids, contact between ridge tops

Pressure & Temperature

Area Bonded

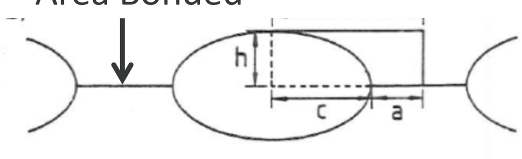

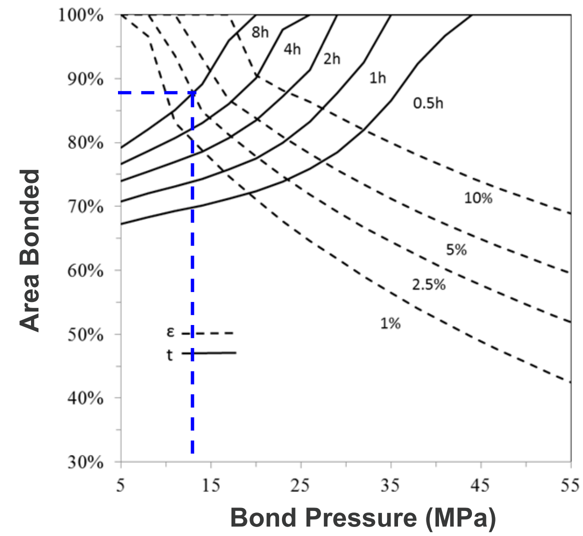

Balance creep, time, pressure and bonded area

- Solid state process
- Applied high pressure at high temperature
- Void closure due to diffusion of constituent atoms and creep processes by application of high pressure

Transient-Liquid-Phase Bonding

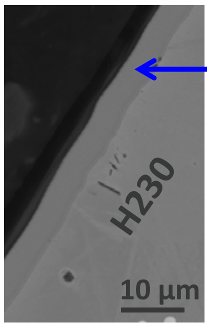

Ni-P plating acts as a low-melting interlayer

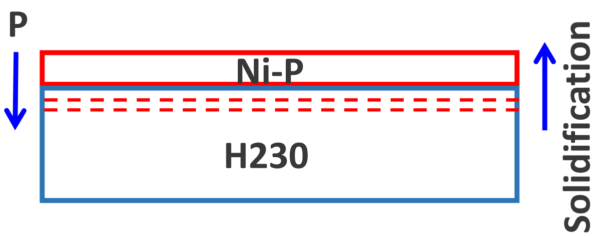

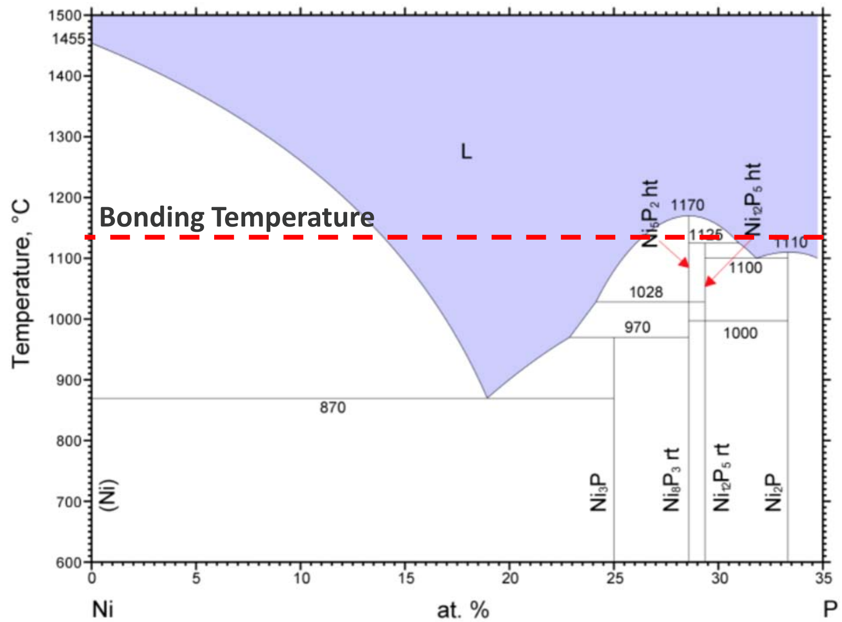

- Both solid state and liquid state reactions
- Less pressure than diffusion bonding
- Lower melting point interlayer
- Isothermal melting and solidification of interlayer

Output of Bonding - stacks

- Downselect between H230 & H282
- H230 – NiCrW solid solution strengthend alloy
- H282 – Gamma prime strengthened alloy
- H230 was selected and challenges with H282 will be discussed later

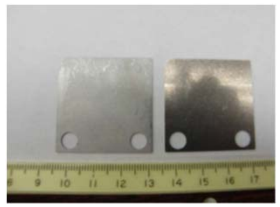

Cold rolled and 1232 °C solution annealed - 550 µm H230 shims

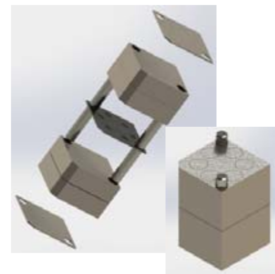

Stacked onto a fixture

Pressed at 1150°C, 12.7MPa in vac

Stacks

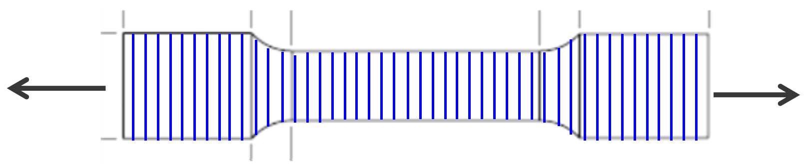

Tensile Samples

Diffusion Bonding of Alloy H230

Microstructure

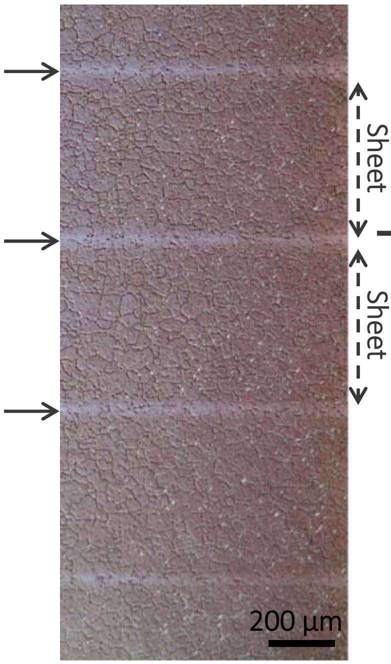

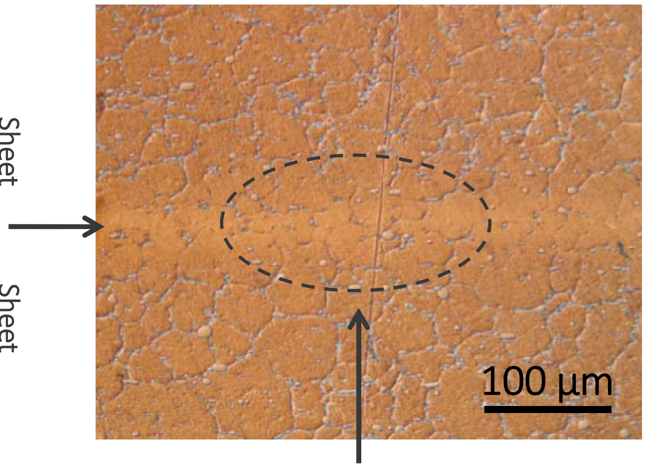

Grain growth

Etched microstructure to observe grain growth through the bond line

Mechanical Behavior

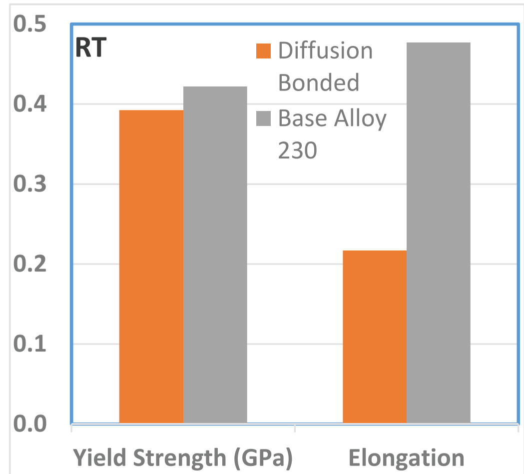

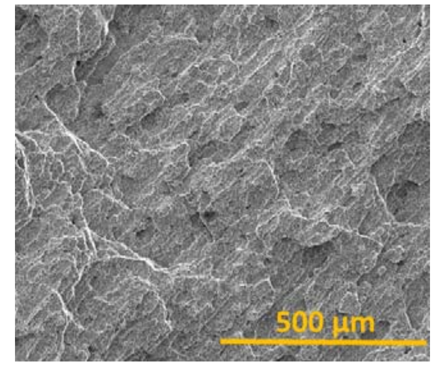

Ductile fracture along the precipitate bands.

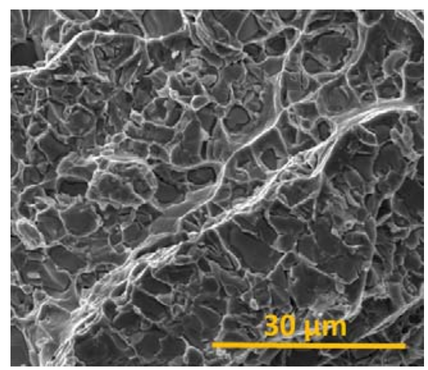

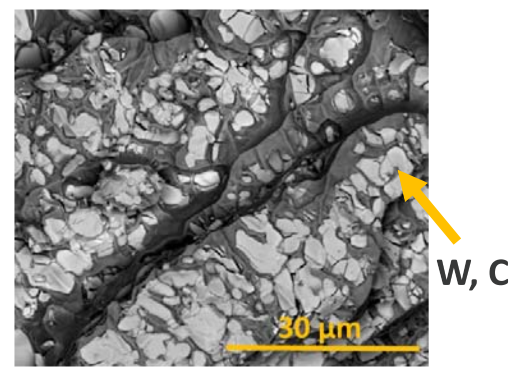

TLP Bonding of Alloy H230

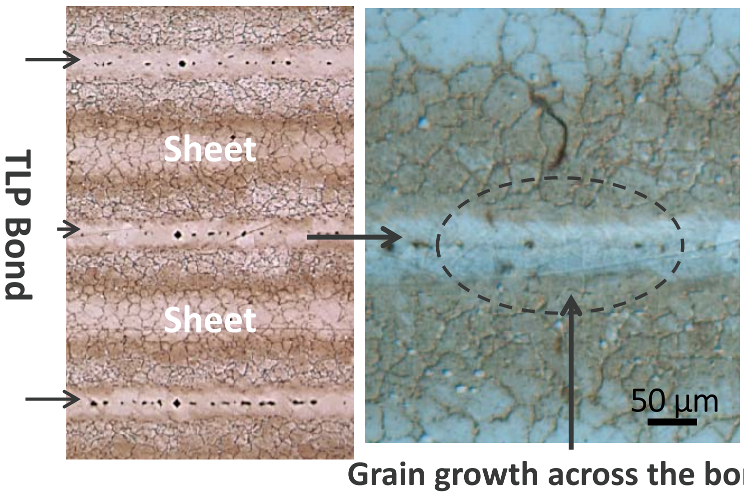

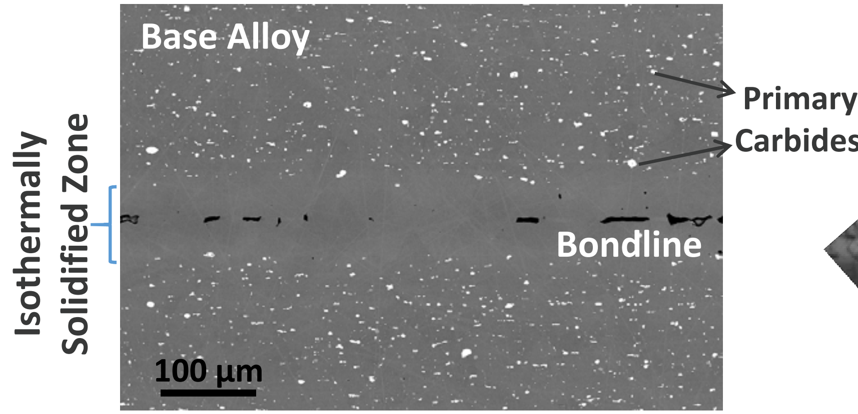

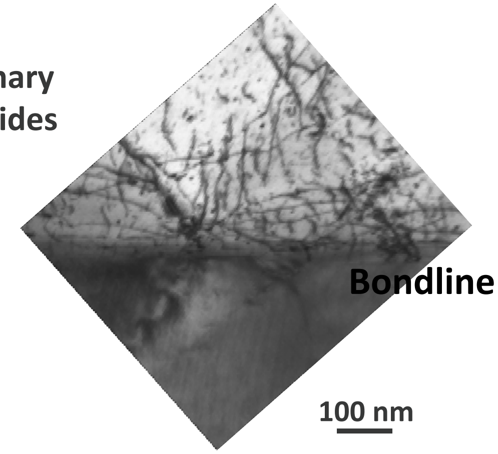

No nanoscale phase near the bondline

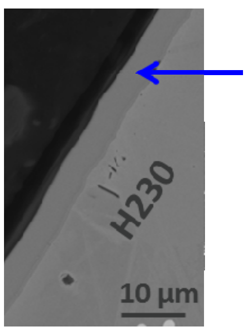

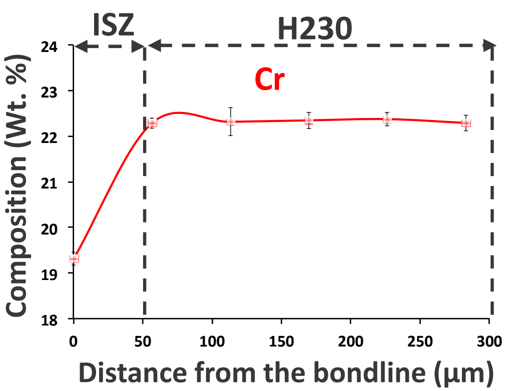

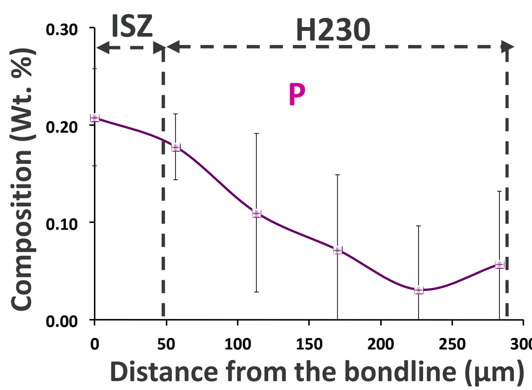

- Cr important for oxidation resistance - Slight reduction in Cr near the bondline
- P should be as low as possible to avoid formation of brittle phases - P is ~0.2 wt. % near the bondline

Tensile Testing

Yield strength of TLP stacks is ~86% of bulk H230

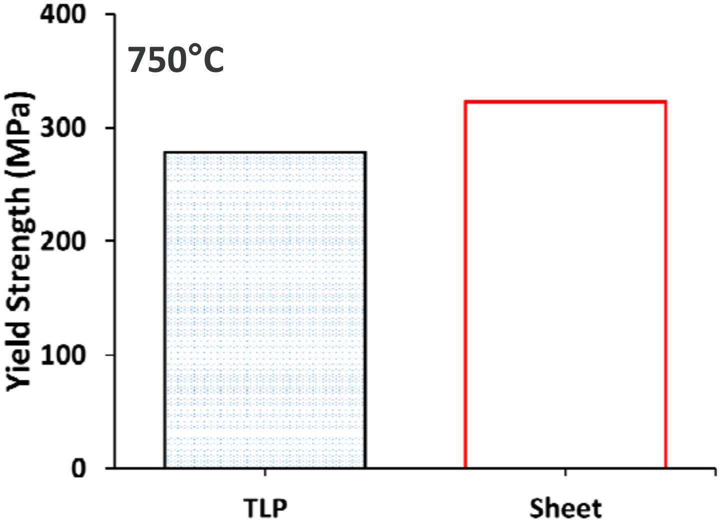

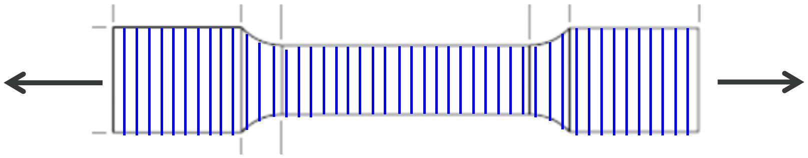

Tensile samples from H230 stacks

Ductile fracture through the ISZ

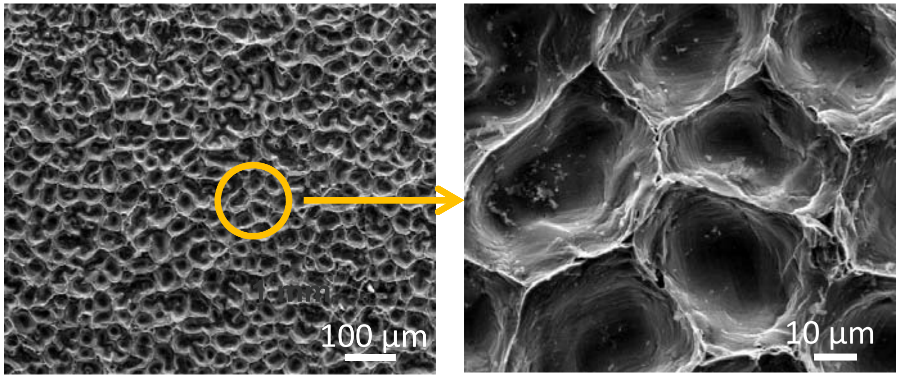

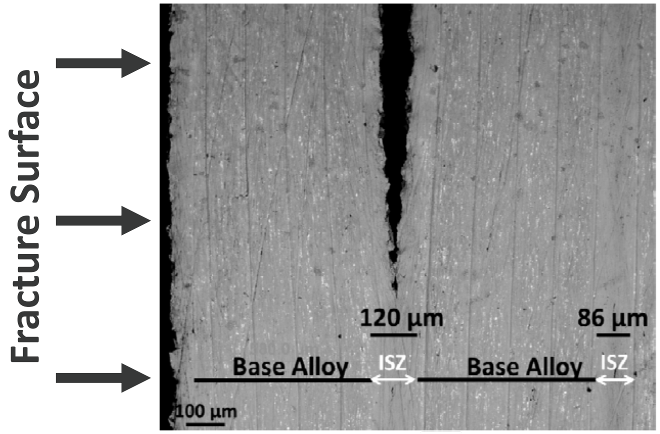

Plastic strain is constrained in the ISZ

High temperature mechanical properties

Creep properties

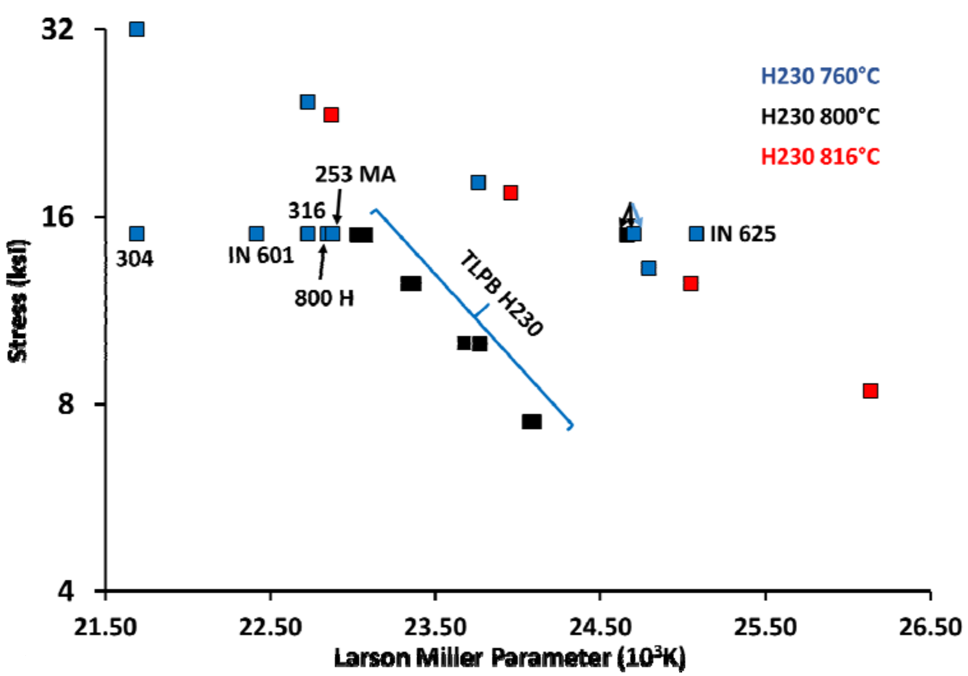

Low cycle fatigue properties @ 760°C

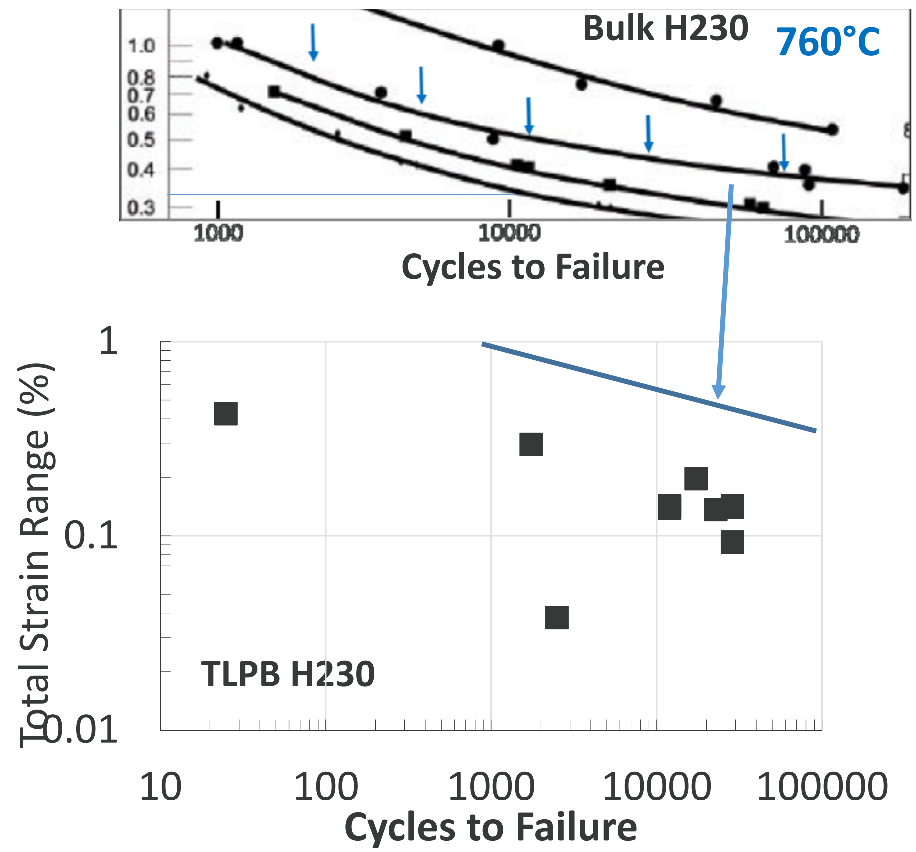

Challenges in bonding of H282

Ni-12P coating on the metal for TLP bonding

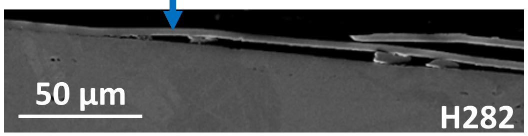

Coating does not adhere to the metal

Bondline after TLP bonding

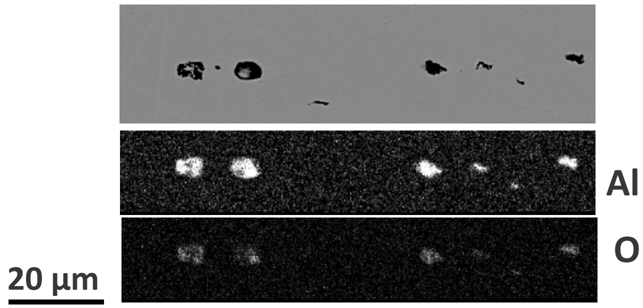

Al_2O_3 particles (dark) along the bondline

Fracture Surface

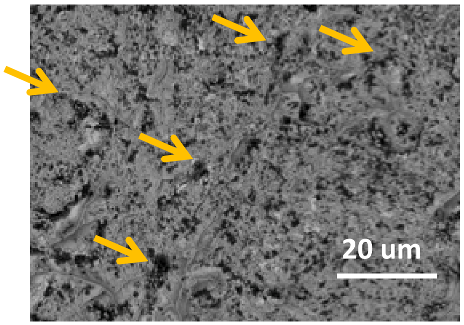

Al_2O_3 particles (dark) on the fracture surface

EDS maps in the vicinity of the bondline

Intermetallic formation

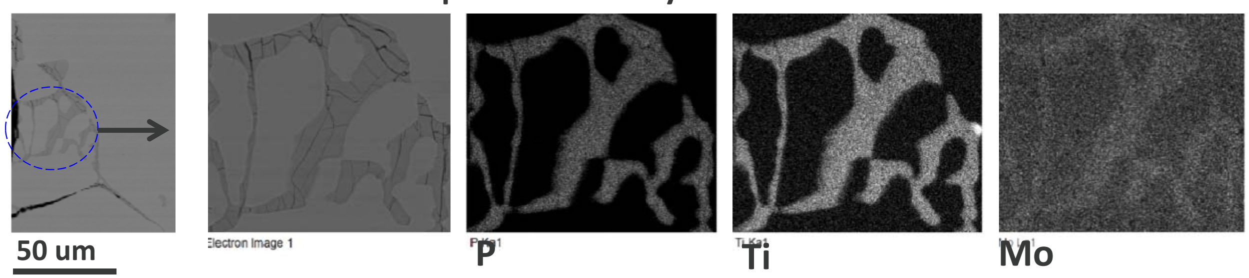

Challenges with TLP bonding of H282 – Surface oxides & Intermetallic Formation

Shrinkage Pores in TLP Bonding

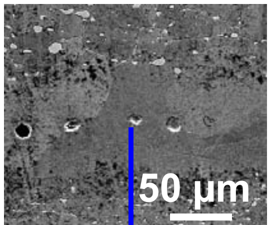

Pores in the vicinity of the bondline with a lamellar structure.

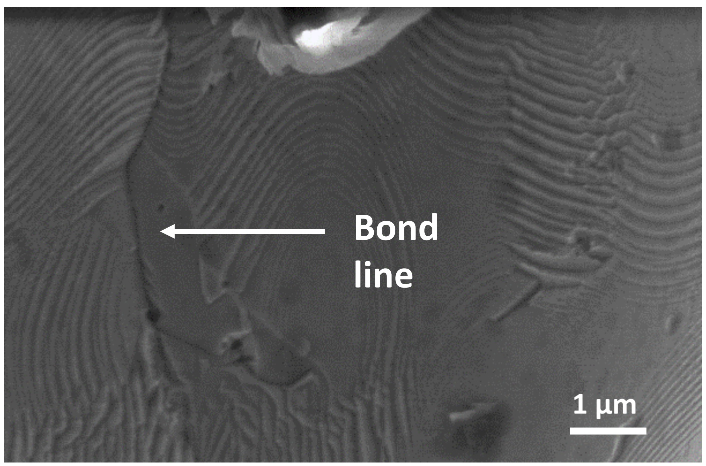

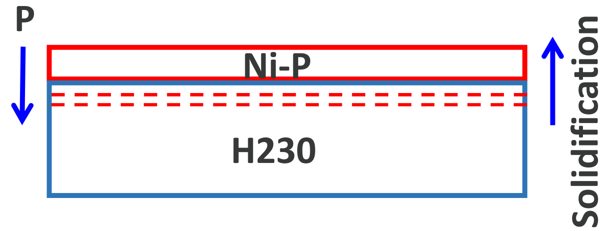

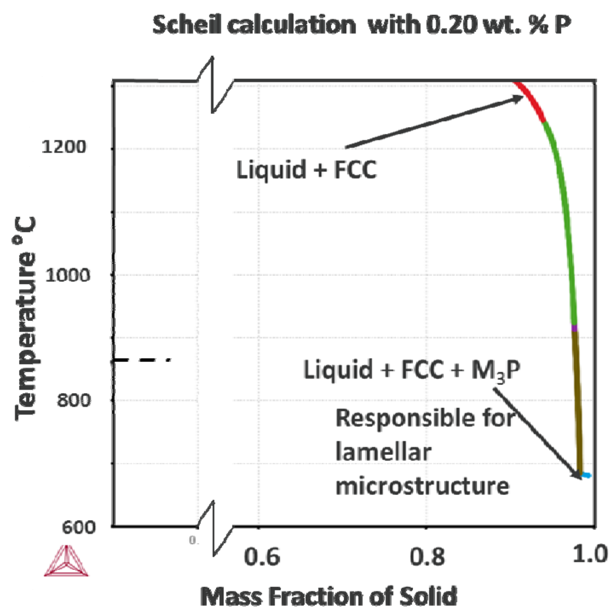

High-Temperature Oxidation of Bonded Regions in CO_2

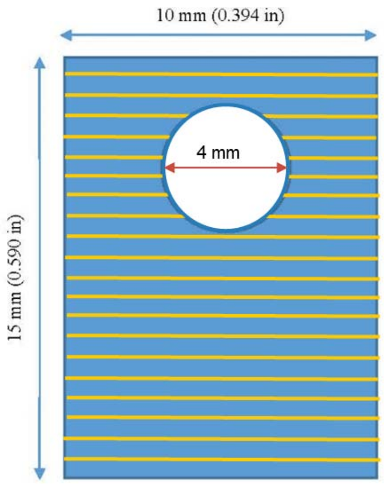

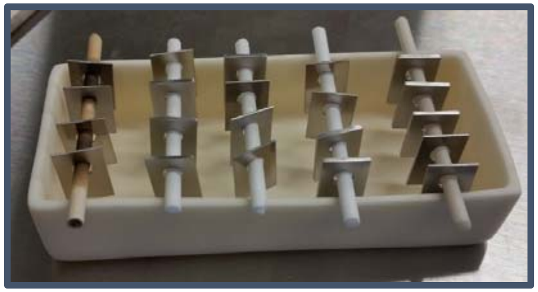

1 bar CO_2 Exposures

- Gas: 1 bar CO_2 (99.999% purity)
- O_2 level in furnace tube: <12 ppm
- Gas flow rate: 0.032 kg/h
- Temperature: 700°C
- Duration: 4000 h in 500 h increments
- 24 h purging with CO_2 before heating

Characterization

Mass Change

XRD

SEM

250 bar CO_2 Exposure

- Gas: CO2 (99.999% purity)
- Flow rate: 2 ml/min
- Temperature: 720°C
- Duration: 1500 h in 500 h incr.
- Argon purging before heating

Oxidation in sCO_2 (720°C – 250 bar)

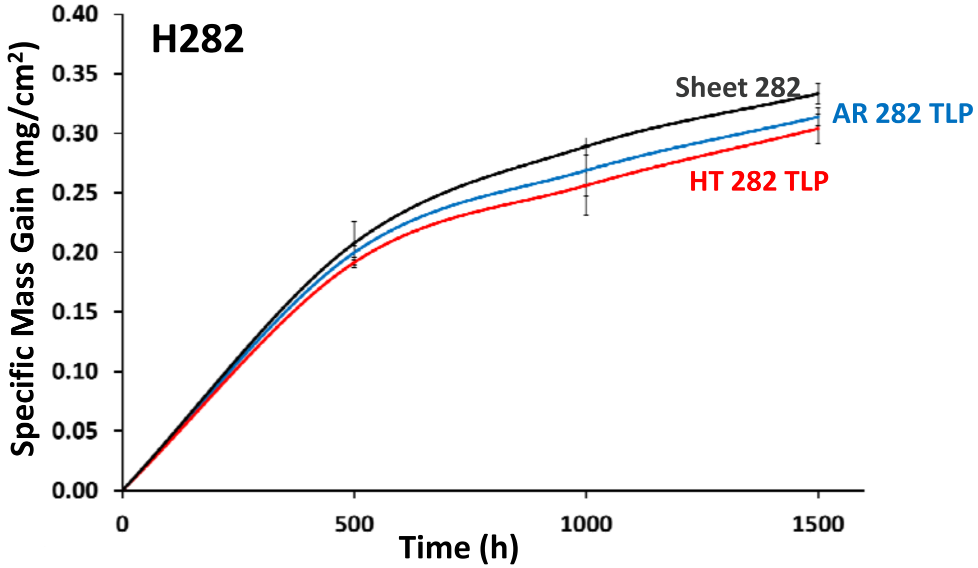

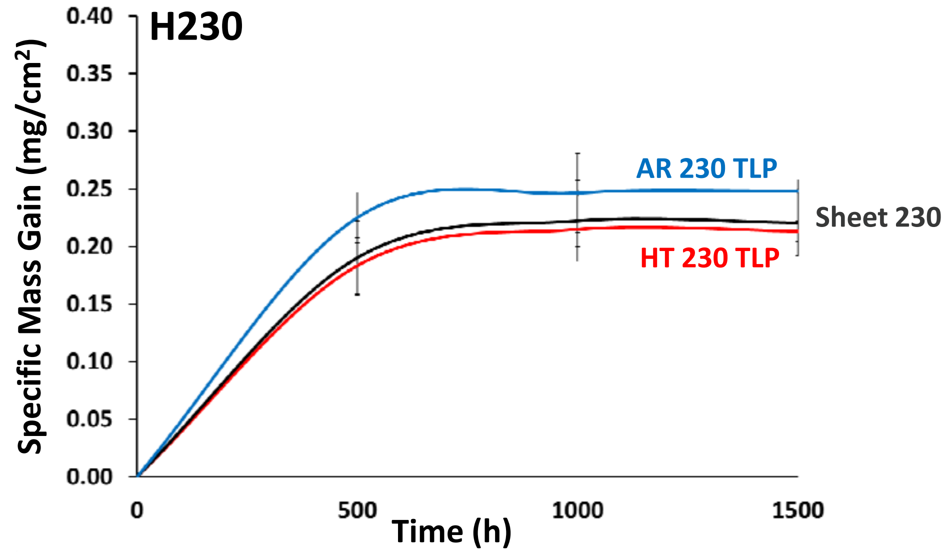

H282 continues to have mass gain up to 1500 hrs BUT H230 mass gain tapers off after 500 hrs

Atmospheric CO_2 Exposure

Fastest oxidation rate within first 500 hrs, then slower, but steady continued oxidation

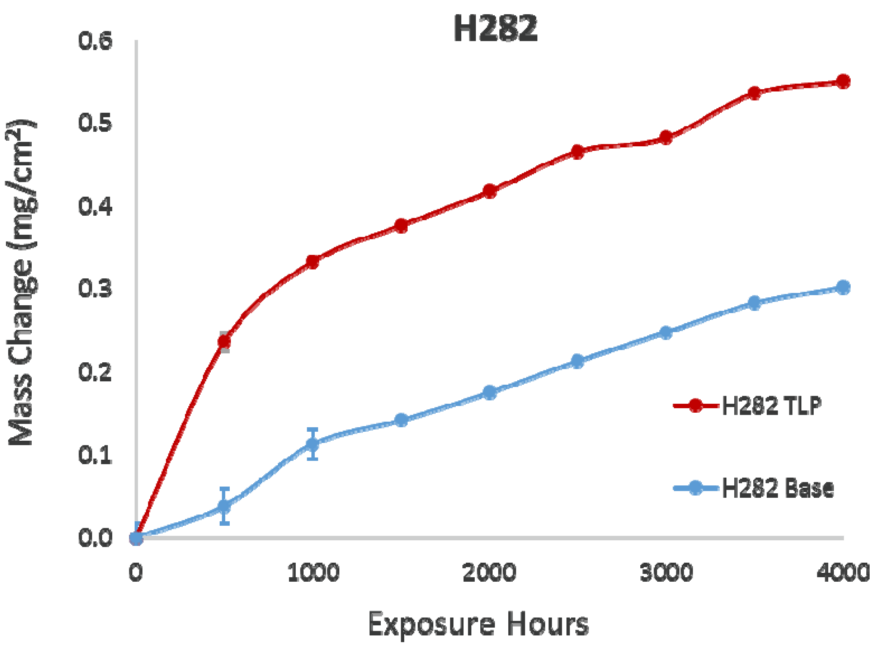

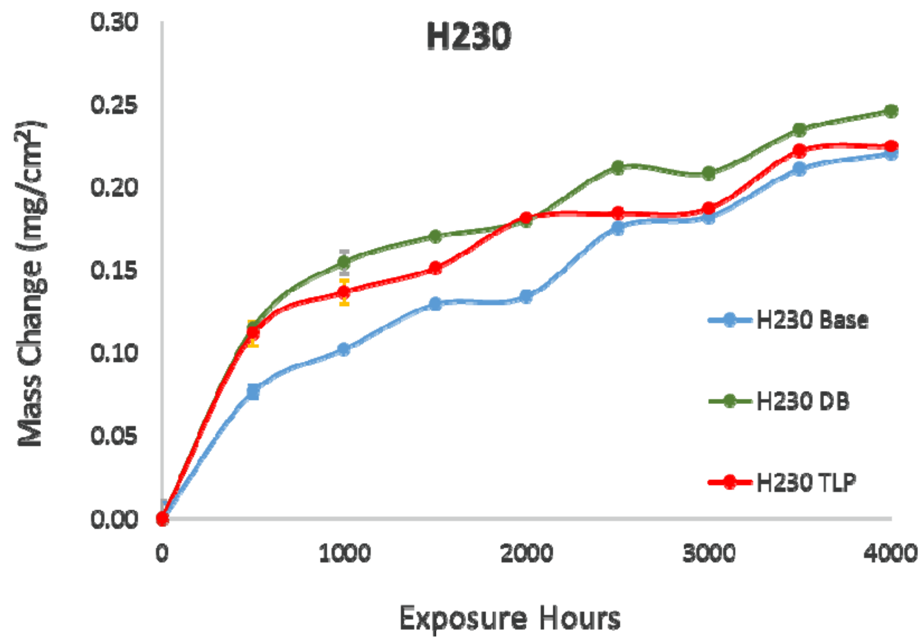

Glancing angle XRD

Surface is predominantly Cr_2O_3, with some M_3O_4 phase appearing at longer exposure times

Surface is primarily Cr_2O_3, with a smaller portion of M_3O_4 phase

Bonded alloys exposed to 700 °C aCO_2

500 h exposure time

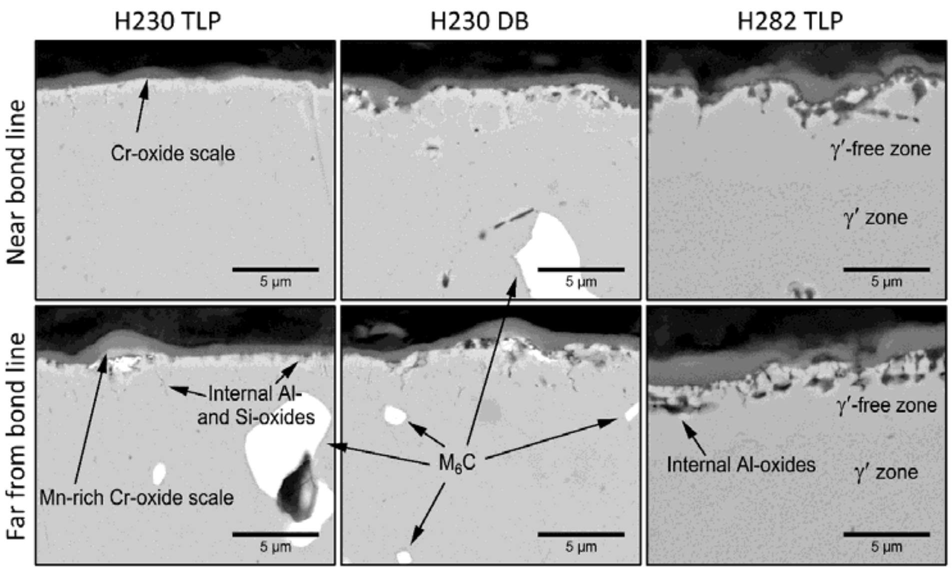

1500 h exposure time

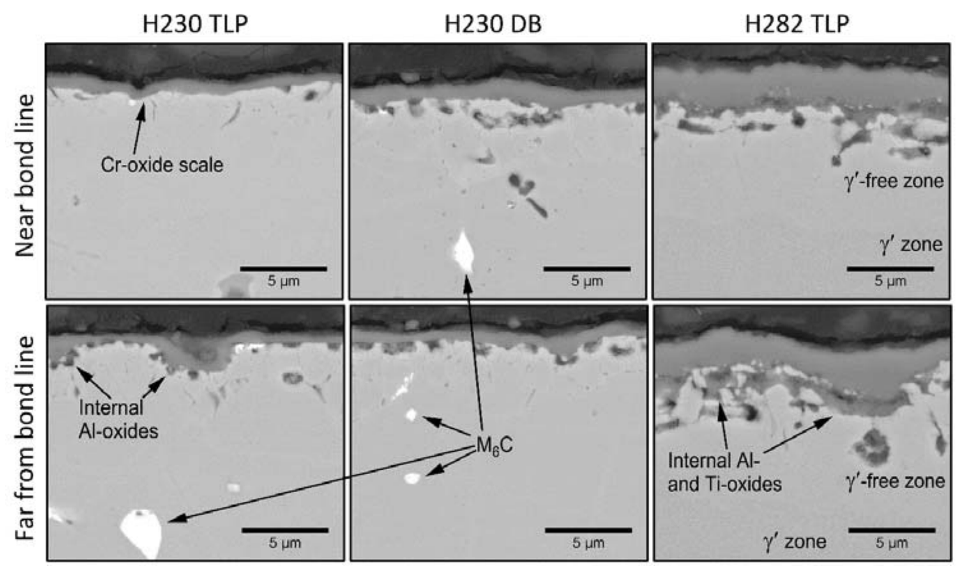

- Thin, protective Cr-rich oxide layers are formed for H230 and H282 during exposure to 700 °C aCO_2.
- Internal oxidation of Al leads to a sub-surface layer depleted of γ' phase in H282.
- No difference in oxidation resistance is observed near/far from the bond layer for either alloy.

Bonded alloys exposed to 720 °C sCO_2

500 h exposure time

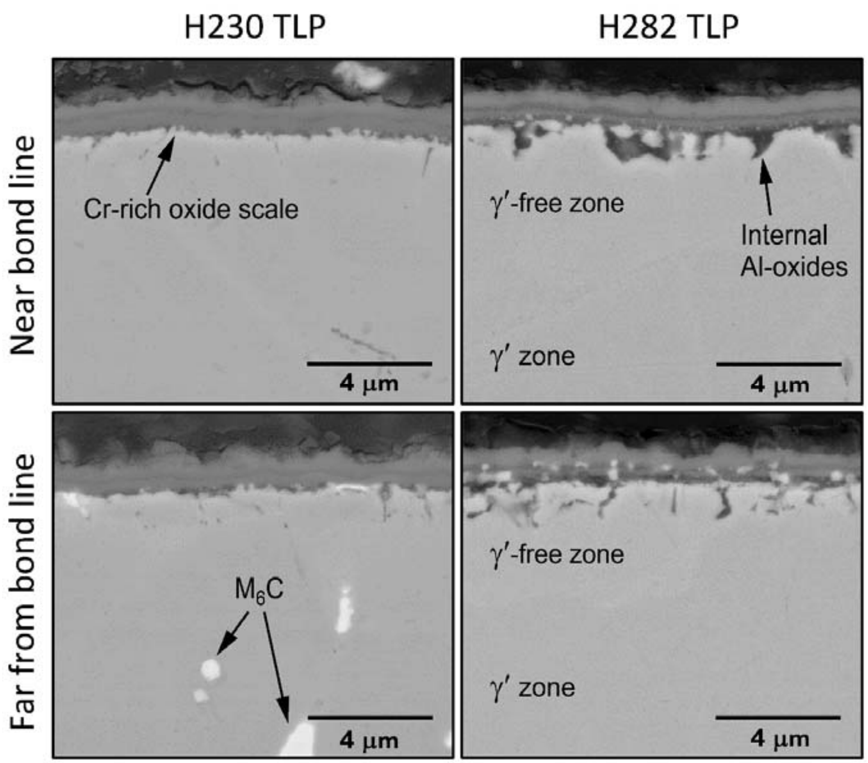

Similar results as H230 and H282 bonded samples exposed to 700 °C aCO_2:

- Thin Cr-rich oxide layers.
- Internal oxidation of Al leads to a sub-surface layer depleted of γ' phase in H282.
- No difference in oxidation resistance observed near/far from the bond layer.

One difference is that sCO_2 exposures show a 2-layer oxide structure containing some Mn (H230) or Ti (H282) in addition to Cr. This is the subject of ongoing investigation.

Performance of welded alloys in sCO_2

- **Similar and dissimilar metal welds (1 inch thick plates) were done with gas tungsten arc welding (GTAW) and post weld heat treated at Edison Welding Institute.**
  - P22 – P22,
  - P91 – P91,
  - 347H – 347H,
  - Alloy 625 – Alloy 625,
  - Alloy 263 – Alloy 263,
  - P22 – P91,
  - P91 – 347H,
  - P22 – Alloy 263,
  - Alloy 625 – Alloy 263 ,
  - 347H – Alloy 263
- **Changes in microstructure (Heat affected zone – HAZ) due to welding were characterized using optical microscopy and hardness testing**
- **sCO2 exposures of weld samples will be performed**
  - Corrosion performance
  - Mechanical performance

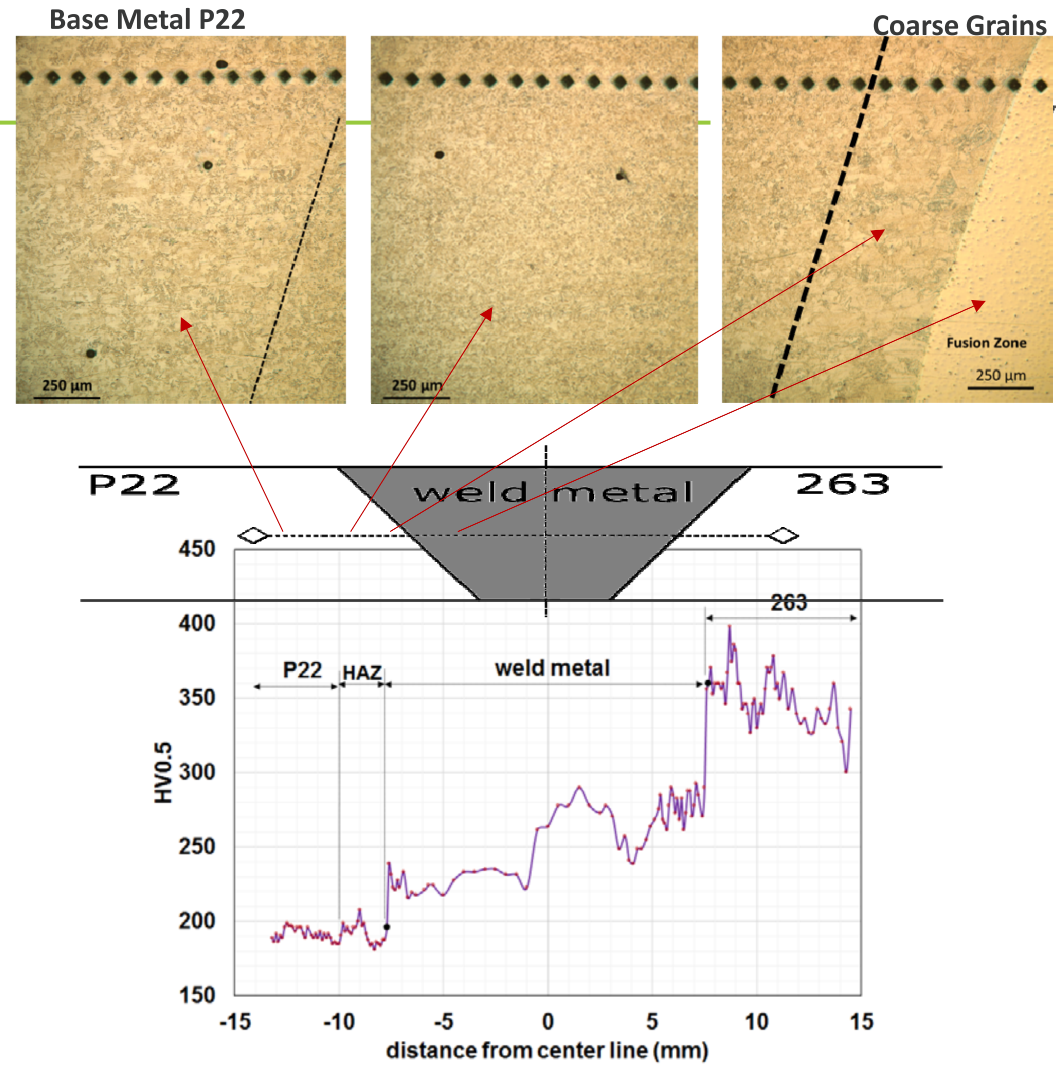

Summary

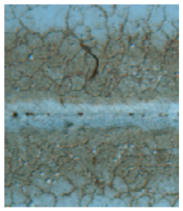

1) Uniform bond with grain growth across the bondline

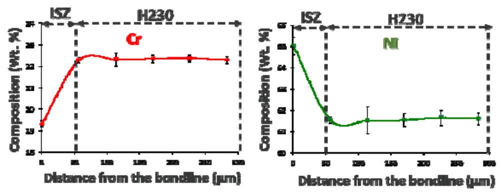

2) Ni increase, Cr dip through the bond

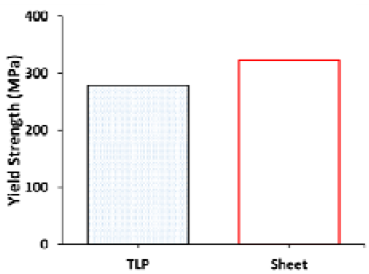

3) TLP-bonded H230 with ~ 86% strength of bulk @ 760°

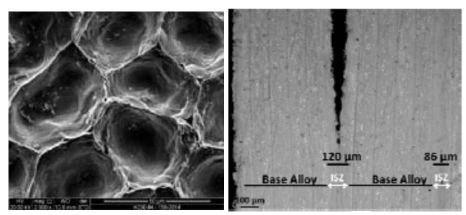

4) Ductile fracture through the bond, plastic strain constrained in the bond region

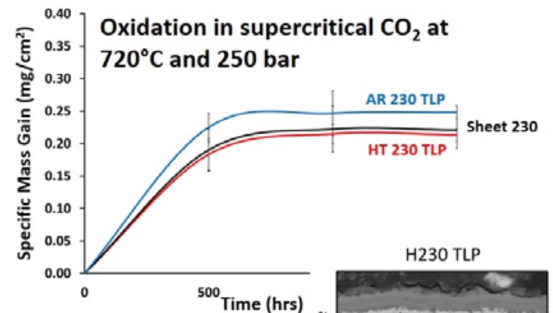

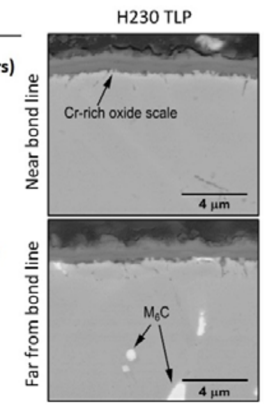

- Thin Cr-rich oxide layers.
- No difference in oxidation resistance observed near/far from the bond layer.

5) Similar oxidation behavior between the bond region and base metal